First results of the ^{230}Th(n,f) cross section measurements at the CERN n_TOF facility

V. Michalopoulou[1,2,*], *A.* Stamatopoulos[2], *R.* Vlastou[2], *M.* Kokkoris[2], *A.* Tsinganis[1], *M.* Diakaki[2,46], *Z.* Eleme[3], *N.* Patronis[3], *J.* Heyse[4], *P.* Schillebeeckx[4], *L.* Tassan-Got[1,2,5], *M.* Barbagallo[1,6], *N.* Colonna[6], *S.* Urlass[1,7], *D.* Macina[1], *E.* Chiaveri[8,9,1], *O.* Aberle[1], *V.* Alcayne[10], *S.* Amaducci[11,12], *J.* Andrzejewski[13], *L.* Audouin[5], *V.* Babiano-Suarez[14], *M.* Bacak[1,15,16], *S.* Bennett[8], *E.* Berthoumieux[16], *D.* Bosnar[17], *A. S.* Brown[18], *M.* Busso[19,20], *M.* Caamaño[21], *L.* Caballero[14], *M.* Calviani[1], *F.* Calviño[22], *D.* Cano-Ott[10], *A.* Casanovas[22], *F.* Cerutti[1], *G. P.* Cortés[22], *M. A.* Cortés-Giraldo[9], *L.* Cosentino[11], *S.* Cristallo[19,23], *L. A.* Damone[6,24], *P. J.* Davies[8], *M.* Dietz[25], *C.* Domingo-Pardo[14], *R.* Dressler[26], *Q.* Ducasse[27], *E.* Dupont[16], *I.* Durán[21], *B.* Fernández-Domíngez[21], *A.* Ferrari[1], *I.* Ferro-Gonçalves[28], *P.* Finocchiaro[11], *V.* Furman[29], *R.* Garg[25], *A.* Gawlik[13], *S.* Gilardoni[1], *K.* Göbel[30], *E.* González-Romero[10], *C.* Guerrero[9], *F.* Gunsing[16], *S.* Heinitz[26], *D. G.* Jenkins[18], *E.* Jericha[15], *U.* Jiri[26], *A.* Junghans[7], *Y.* Kadi[1], *F.* Käppeler[31], *A.* Kimura[32], *I.* Knapová[33], *Y.* Kopatch[29], *M.* Krtička[33], *D.* Kurtulgil[30], *I.* Ladarescu[14], *C.* Lederer-Woods[25], *J.* Lerendegui-Marco[9], *S. -J.* Lonsdale[25], *A.* Manna[34,35], *T.* Martínez[10], *A.* Masi[1], *C.* Massimi[34,35], *P. F.* Mastinu[36], *M.* Mastromarco[1,8], *E.* Maugeri[26], *A.* Mazzone[6,37], *E.* Mendoza[10], *A.* Mengoni[38,34], *P. M.* Milazzo[39], *M. A.* Millán-Callado[9], *F.* Mingrone[1], *J.* Moreno-Soto[16], *A.* Musumarra[11,12], *A.* Negret[40], *F.* Ogállar[41], *A.* Oprea[40], *A.* Pavlik[42], *J.* Perkowski[13], *C.* Petrone[40], *L.* Piersanti[19,23], *E.* Pirovano[27], *I.* Porras[41], *J.* Praena[41], *J. M.* Quesada[9], *D.* Ramos Doval[5], *R.* Reifarth[30], *D.* Rochman[26], *C.* Rubbia[1], *M.* Sabaté-Gilarte[9,1], *A.* Saxena[43], *D.* Schumann[26], *A.* Sekhar[8], *A. G.* Smith[8], *N.* Sosnin[8], *P.* Sprung[26], *G.* Tagliente[6], *J. L.* Tain[14], *A. E.* Tarifeño-Saldivia[22], *B.* Thomas[30], *P.* Torres-Sánchez[41], *S.* Valenta[33], *G.* Vannini[34,35], *V.* Variale[6], *P.* Vaz[28], *A.* Ventura[34], *D.* Vescovi[19,44], *V.* Vlachoudis[1], *A.* Wallner[45], *P. J.* Woods[25], *T. J.* Wright[8], and *P.* Žugec[17]

[1]European Organization for Nuclear Research (CERN), Switzerland
[2]National Technical University of Athens, Greece
[3]University of Ioannina, Greece
[4]European Commission, Joint Research Centre, Geel, Retieseweg 111, B-2440 Geel,Belgium
[5]IPN, CNRS-IN2P3, Univ. Paris-Sud, Université Paris-Saclay, F-91406 Orsay Cedex,France
[6]Istituto Nazionale di Fisica Nucleare, Bari, Italy
[7]Helmholtz-Zentrum Dresden-Rossendorf, Germany
[8]University of Manchester, United Kingdom
[9]Universidad de Sevilla, Spain
[10]Centro de Investigaciones Energéticas Medioambientales y Tecnológicas (CIEMAT),Spain
[11]INFN Laboratori Nazionali del Sud, Catania, Italy
[12]Dipartimento di Fisica e Astronomia, Università di Catania, Italy
[13]University of Lodz, Poland
[14]Instituto de Física Corpuscular, CSIC - Universidad de Valencia, Spain
[15]Technische Universität Wien, Austria
[16]CEA Saclay, Irfu, Université Paris-Saclay, Gif-sur-Yvette, France
[17]Department of Physics, Faculty of Science, University of Zagreb, Croatia
[18]University of York, United Kingdom
[19]Istituto Nazionale di Fisica Nazionale, Perugia, Italy
[20]Dipartimento di Fisica e Geologia, Università di Perugia, Italy
[21]University of Santiago de Compostela, Spain
[22]Universitat Politècnica de Catalunya, Spain
[23]Istituto Nazionale di Astrofisica - Osservatorio Astronomico d'Abruzzo, Italy
[24]Dipartimento di Fisica, Università degli Studi di Bari, Italy
[25]School of Physics and Astronomy, University of Edinburgh, United Kingdom
[26]Paul Scherrer Institut (PSI), Villigen, Switzerland
[27]Physikalisch-Technische Bundesanstalt (PTB), Bundesallee 100, 38116 Braunschweig, Germany
[28]Instituto Superior Técnico, Lisbon, Portugal
[29]Joint Institute for Nuclear Research (JINR), Dubna, Russia
[30]Goethe University Frankfurt, Germany
[31]Karlsruhe Institute of Technology, Campus North, IKP, 76021 Karlsruhe, Germany
[32]Japan Atomic Energy Agency (JAEA), Tokai-mura, Japan
[33]Charles University, Prague, Czech Republic

[34]Istituto Nazionale di Fisica Nucleare, Sezione di Bologna, Italy
[35]Dipartimento di Fisica e Astronomia, Università di Bologna, Italy
[36]Istituto Nazionale di Fisica Nucleare, Sezione di Legnaro, Italy
[37]Consiglio Nazionale delle Ricerche, Bari, Italy
[38]Agenzia nazionale per le nuove tecnologie, l'energia e lo sviluppo economico sostenibile (ENEA), Bologna, Italy
[39]Istituto Nazionale di Fisica Nazionale, Trieste, Italy
[40]Horia Hulubei National Institute of Physics and Nuclear Engineering (IFIN-HH),Bucharest
[41]University of Granada, Spain
[42]University of Vienna, Faculty of Physics, Vienna, Austria
[43]Bhabha Atomic Research Centre (BARC), India
[44]Gran Sasso Science Institute (GSSI), L'Aquila, Italy
[45]Australian National University, Canberra, Australia
[46]CEA, Cadarache, DEN/DER/SPRC/LEPh, 13108 Saint Paul Les Durance, France

Abstract. The study of neutron-induced reactions on actinides is of considerable importance for the design of advanced nuclear systems and alternative fuel cycles. Specifically, ^{230}Th is produced from the α-decay of ^{234}U as a byproduct of the ^{232}Th/^{233}U fuel cycle, thus the accurate knowledge of its fission cross section is strongly required. However, few experimental datasets exist in literature with large deviations among them, covering the energy range between 0.2 to 25 MeV. In addition, the study of the ^{230}Th(n,f) cross-section is of great interest in the research on the fission process related to the structure of the fission barriers. Previous measurements have revealed a large resonance at E_n=715 keV and additional fine structures, but with high discrepancies among the cross-section values of these measurements. This contribution presents preliminary results of the ^{230}Th(n,f) cross-section measurements at the CERN n_TOF facility. The high purity targets of the natural, but very rare isotope ^{230}Th, were produced at JRC-Geel in Belgium. The measurements were performed at both experimental areas (EAR-1 and EAR-2) of the n_TOF facility, covering a very broad energy range from thermal up to at least 100 MeV. The experimental setup was based on Micromegas detectors with the ^{235}U(n,f) and ^{238}U(n,f) reaction cross-sections used as reference.

1 Introduction

The Th/U fuel cycle has several advantages concerning radioactive waste management and non-proliferation, compared with the conventional U-Pu fuel cycle [1]. In order to achieve improved design calculations for thorium based reactors, the determination of neutron induced reaction cross-sections on isotopes of thorium is required.

Specifically, the ^{230}Th isotope is produced from the α-decay of ^{234}U as a byproduct of the ^{232}Th/^{233}U fuel cycle. Regarding ^{230}Th(n,f) cross-section, the existing experimental datasets cover the energy range between 0.2 to 25 MeV with large deviations among them. Furthermore, interesting structures appear in the cross section of this isotope at the fission barrier, giving insight to the fission potential wells. In this context, the ^{230}Th(n,f) cross-section was measured at the CERN n_TOF facility, with the aim of covering with high accuracy data over a broad energy range from thermal up to at least 100 MeV.

The measurement was performed with the same experimental setup at both experimental areas EAR-1 [2] and EAR-2 [3] of the CERN n_TOF facility, exploiting their different neutron beam characteristics, in order to cover the largest possible energy range and minimize the systematic uncertainties of the final cross-section results. In the present contribution, the experimental setup and the analysis, along with first results above ~500keV, will be presented and discussed.

*e-mail: veatriki.michalopoulou@cern.ch

2 Experimental setup

2.1 The n_TOF facility

The measurement was performed at the experimental areas EAR-1 and EAR-2 of the CERN n_TOF facility. Neutrons are produced by proton-induced spallation on a lead target with energies ranging from thermal up to the GeV region. In order to reach the experimental areas, the neutrons travel flight paths of 185 m horizontally and 19.5 m vertically to EAR-1 and EAR-2, respectively. This difference in the flight paths results in different neutron beam characteristics in the two experimental areas.

Specifically, experimental area EAR-1 offers better neutron energy resolution combined with the capability to reach higher neutron energies, while experimental area EAR-2 offers a higher neutron flux [4]. The experimental setups at experimental areas EAR-1 and EAR-2 are shown in Figure 1 and Figure 2 respectively.

2.2 Samples

Seven high purity thorium samples, prepared at JRC-Geel, were used for the measurements, with a total ^{230}Th mass of ~32 mg , while ~3.6 mg ^{235}U and ~14.4 mg ^{238}U samples were used as references. The material was deposited on a 0.025 mm thick aluminum backing in the form of 8 cm diameter disks.

In the thorium samples, Pu contaminants which have a significant contribution in the yield below the fission threshold were present and need to be considered in the analysis. A detailed characterization of the thorium and

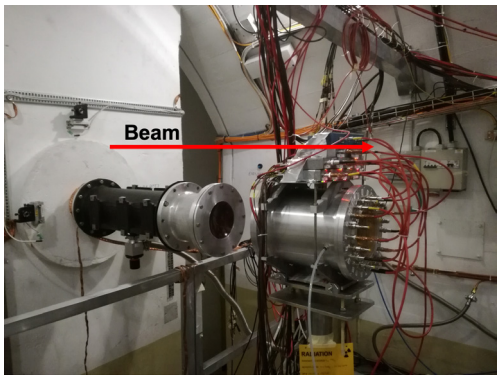

Figure 1. The fission chamber inside the experimental area EAR-1. The arrow indicates the direction of the neutron beam.

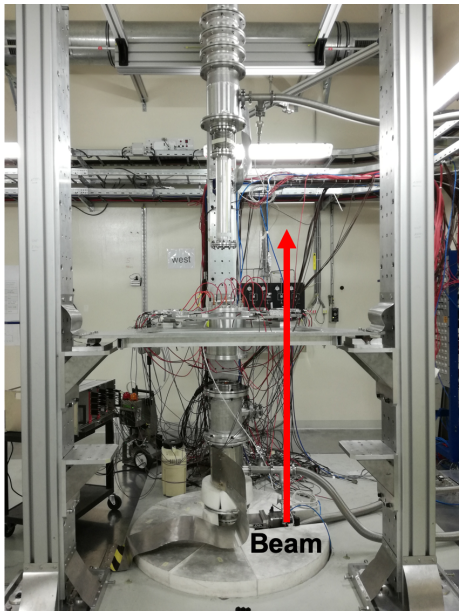

Figure 2. The fission chamber inside the experimental area EAR-2. The arrow indicates the direction of the neutron beam.

uranium samples is ongoing, thus, the mass and contaminants of the samples are currently known with a high uncertainty.

2.3 Detectors

The measurements were carried out using a set-up based on Micro-Bulk Micromegas (Micro-Mesh Gaseous Structure) detectors [5]. The detector volume is divided into two parts by a thin electrode with holes, called micromesh: the drift region with an electric field of ~1kV/cm and the amplification region with an electric field of ~50 kV/cm. The samples and detectors were placed in pairs, as shown in Figure 3, in an aluminum chamber filled with a mixture of Ar:CF_4:isoC_4H_{10} (88:10:2) at atmospheric pressure and room temperature.

The actinide samples act as the drift electrode of each detector. When a fission event occurs the heavy and the light fission fragments move in opposite directions due to the kinematics of the reaction, one of the two entering the drift region of the detector, while the other is not detected. In the drift region the fission fragment creates primary electrons, which are guided towards the mesh electrode from the electric field applied. Upon entering the mesh region the electrons are multiplied. The positive ions created in the amplification region are collected from the mesh and result in the formation of the signals. A schematic representation of the operating principle of the Micromegas detector is shown in Figure 4.

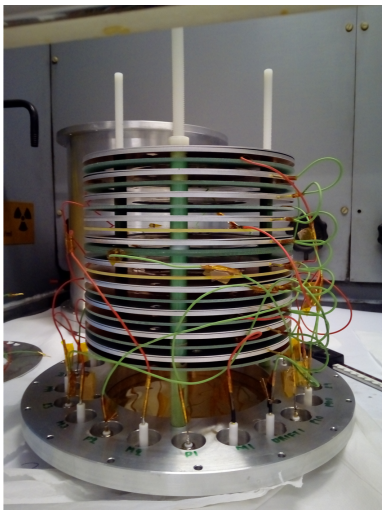

Figure 3. The samples and Micromegas detectors setup, inside the fission chamber.

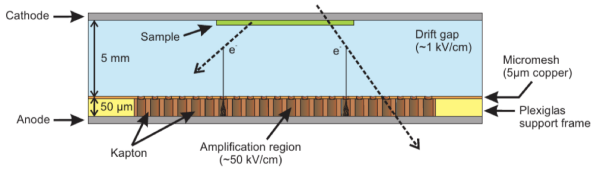

Figure 4. A schematic representation of the Micromegas detector. The primary electrons drift towards the mesh electrode and are multiplied in the mesh region. The signal is collected from the mesh electrode.

3 Data analysis

The detector signals were digitized and then analyzed by means of a pulse shape recognition routine [6], in order to determine the amplitude of each pulse and its arrival time, which is correlated to the energy of the neutron that caused the fission event. Data without the neutron beam were regularly recorded in order to a) check the stability of the detectors and b) determine the amplitude distributions which originate from the alpha activity of the targets. Depending on the amplitude, each pulse is either attributed to the alpha activity of the samples or to a fission event. Fission signals with an amplitude lower than the applied pulse-height threshold are rejected, in order to completely reject the alpha counts from the analysis. The fraction of

these rejected fission events is estimated by FLUKA [7, 8] simulations of the detector, using the GEF [9] code as a fission event generator. This work is in progress, while a typical experimental pulse height spectrum is shown in Figure 5.

The arrival time of each signal is determined relative to the "γ-flash" signal. In addition to neutrons, the interaction of the protons with the lead target results in the production of γ-rays and other relativistic particles which reach the experimental areas at (almost) the speed of light. This "γ-flash" causes a high amplitude signal, lasting a few hundred ns. In order to mitigate this effect, an average "γ-flash" shape is calculated for all detectors separately, as shown Figure 6. The average "γ-flash" shape is subtracted from each event and normalized to the amplitude of the pulse. The energy of the neutron that caused the fission event is calculated from the time of flight difference between the "γ-flash" and the fission pulse.

The ^{230}Th(n,f) cross-section was calculated using the ^{235}U(n,f) and ^{238}U(n,f) reactions as references, assuming all targets receive the same flux. Since the final mass of the targets and the contaminants characterization is in progress, and the correction for the fission fragments which are recorded below the amplitude threshold is not yet finalized, the cross-section results presented are preliminary.

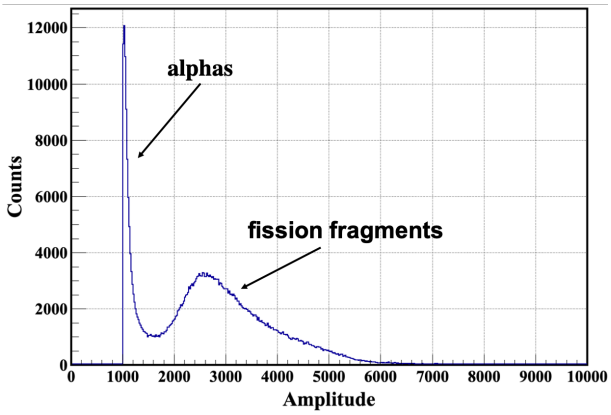

Figure 5. Experimental pulse height spectrum for ^{230}Th.

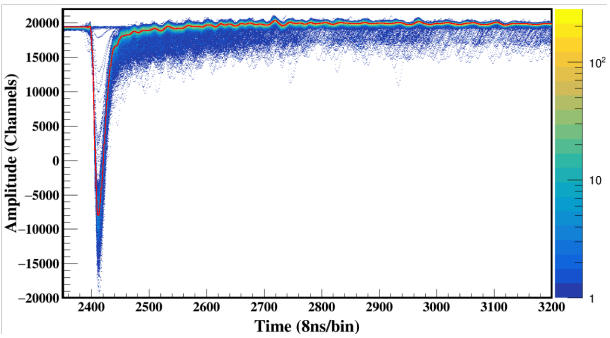

Figure 6. Average "γ-flash" shape (red) calculated from raw "γ-flash" pulses for ^{230}Th.

4 Results

The preliminary ^{230}Th(n,f) cross-section results, with the ^{235}U(n,f) cross-section used as reference, deduced as the mean value from the seven thorium targets up to 100 MeV are presented in Figure 7, along with the previous datasets. As seen in Figure 7 the preliminary cross-section results are in agreement within errors with the data from Muir and Vesser [17] at the region of the resonance (from 650 to 840 keV). For energies higher than 800 keV the cross-section results are in agreement within errors with the data from Meadows [14], as well as with the data from Muir and Vesser, with exception of the energy region between 840 keV to 1 MeV. Regarding the data from the surrogate method from Goldblum *et al.* [10] and Petit *et al.* [11], the cross-section results are in good agreement within errors for energies higher than 1 MeV, while for energies higher than 7 MeV the data from Petit *et al.* are systematically lower and for energies higher than 22 MeV the data from Goldblum *et al.* [10] are systematically higher than the present data. Large deviations are observed between the present data and the data of Boldeman and Walsh [13], Blons *et al.* [15], James *et al.* [16] and Kazarinova *et al.* [18] at the resonance region until 4 MeV. At the energy of ~14 MeV the present data are in agreement within errors with the available data points of Meadows [12], Kazarinova *et al.* and Goldblum *et al.*.

For energies higher than ~30 MeV additional corrections are required and have not yet been applied to the data, such as dead time correction, while the "γ-flash" subtraction routine is more important to this high energy region. The preliminary cross-section results up to 100 MeV for the ^{230}Th(n,f) reaction are presented in Figure 8 along with the latest evaluations ENDF/B-VIII.0 [19] which adopts the JENDL-4.0 [21] evaluation, JEFF-3.3 [20] and TENDL-2017 [22]. As seen in Figure 8 the cross-section from the present work is in agreement with the JENDL-4.0 (ENDF/B-VIII.0) evaluation up to 7 MeV and from 14 MeV up to 20 MeV. In the energy range between 7 and 14 MeV, the shape of the cross-section in this work differs from the latest evaluations, having a dip in the cross-section value at ~13 MeV, while the JENDL-4.0 (ENDF/B-VIII.0), JEFF-3.3 and TENDL-2017 evaluations have local maximum at approximately the same energy. For energies higher than 20 MeV the only available evaluation is TENDL-2017, but the discrepancies with the present data regarding both the shape and the cross-section value are significant.

The analysis of the high energy region from the experimental area EAR-1 measurement is in progress in order to extend the results to higher energies and to estimate the necessary correction factors such as amplitude cut correction, dead time, contribution from contaminants etc. Regarding the EAR-2 measurement, the analysis is ongoing, in order to correct for the plutonium contaminants, present in the ^{230}Th samples, which dominate the yield below the fission threshold.

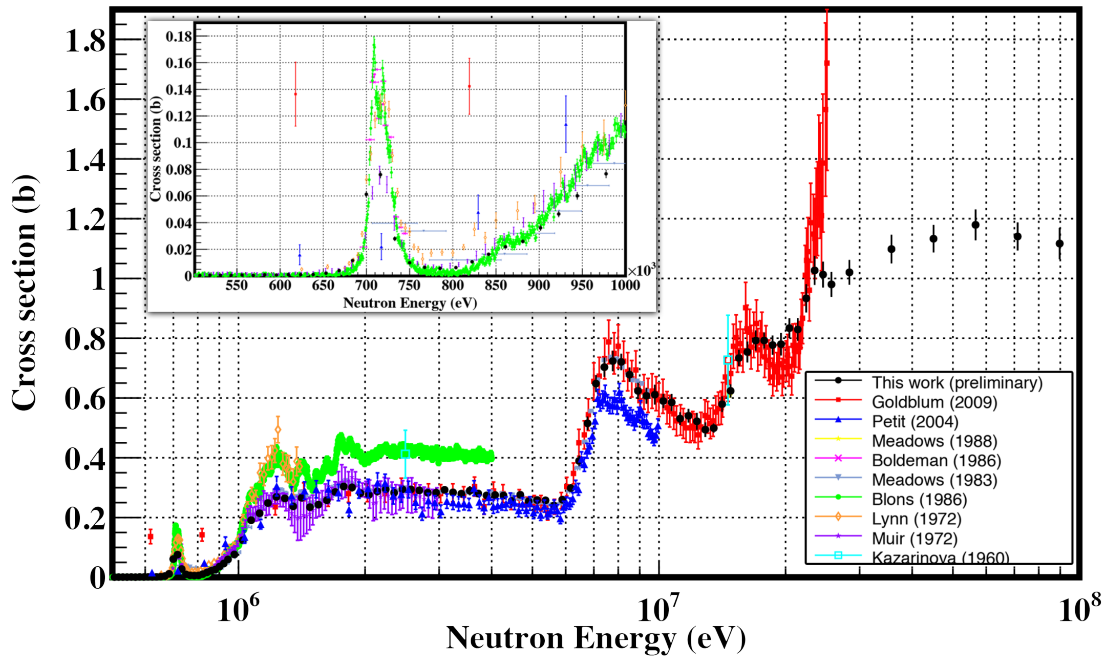

Figure 7. Preliminary cross-section results, mean from seven ^{230}Th targets, up to 100 MeV for ^{230}Th(n,f) reaction (black points), statistical errors only, in comparison to experimental datasets from EXFOR. The inset contains the same plot zoomed in the threshold region.

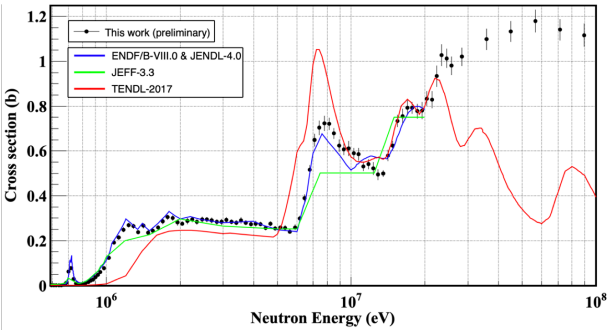

Figure 8. Preliminary cross-section results up to 100 MeV for ^{230}Th(n,f) reaction (black points), statistical errors only, in comparison to the latest evaluated libraries ENDF/B-VIII.0 which adopts the JENDL-4.0 library (blue), JEFF-3.3 (green) and TENDL-2017 (red).

5 Conclusions

The ^{230}Th(n,f) measurement was performed at the experimental areas EAR-1 and EAR-2 at CERN's n_TOF facility and preliminary cross-section results in the energy range between 600 keV to 100 MeV are presented. The analysis is ongoing but the measurement at both experimental areas is expected to cover a very wide energy range, taking advantage of the substantially better energy resolution of EAR-1 to measure the high energy region, and the higher neutron flux of EAR-2 to measure the lower energy region, where the cross-section is expected to be small. The data from the present work will provide for the first time results at energies higher than 25 MeV and useful information for the improvement of the evaluations.

References

[1] D.N. Suglobov et al., Radiochem. **49**, 441-448 (2007)
[2] C. Guerrero et al., Eur. Phys. J. A **49**, 27-41 (2013)
[3] C. Weiß et al., Nucl. Instrum. Meth. A **799**, 90-98 (2015)
[4] M. Sabaté-Gilarte et al., Eur. Phys. J. A **53**, 210 (2017)
[5] S. Andriamonje et al., J. Korean Phy. Soc. **59**, 1597 (2011)
[6] P. Žugec et al., Nucl. Instrum. Meth. A **812**, 134 (2016)
[7] A. Ferrari et al., CERN-2005-010 (2005)
[8] T.T. Böhlen et al., Nucl. Data Sheets **120**, 211 (2014)
[9] K.-H. Schmidt et al., Nucl. Data Sheets **131**, 107 (2016)
[10] B.L. Goldblum et al., Phys. Rev. C **80**, 044610 (2009)
[11] M. Petit et al., Nucl. Phys. A **735**, 345 (2004)
[12] J.W. Meadows, Annals of Nuclear Energy **15**, 421 (1988)
[13] J.W. Boldeman and R.L. Walsh, Radiation Effects **92**, 317 (1986)
[14] J.W. Meadows, Argonne National Laboratory Reports, No.83 (1983)
[15] J. Blons et al., Proceedings of the 18th International Winter Meeting on Nuclear Physics, CEA-CONF-5122, Bormio (1980)

[16] G.D. James et al., Nucl. Phys. A **189**, 225 (1972)
[17] D.W. Muir and L.R.Vesser, 3rd Conf. Neutron Cross-Sections and Tech., Knoxville **1**, 292 (1971)
[18] M.I. Kazarinova et al., Atomnaya Energiya **8**, 139 (1960)
[19] D.A. Brown et al., Nucl. Data Sheets **148**, 1 (2018)
[20] JEFF-3.3: Evaluated Data Library 2017, http://www.oecd-nea.org/dbdata/jeff/jeff33/
[21] K. Shibata et al., Nucl. Sci. Tech. **48**, 1 (2011)
[22] A.J. Koning and D. Rochman, Nucl. Data Sheets **113**, 2841 (2012)